

Design, Synthesis, Biological Evaluation, and Molecular Docking of Novel Benzopyran and Phenylpyrazole Derivatives as Akt Inhibitors

Wenhu Zhan², Sendong Lin², Jing Chen³, Xiaowu Dong², Jianbo Chu¹ and Wenting Du^{1,*}

¹Department of Pharmacy, Zhejiang Medical College, 481 Binwen Road, Hangzhou 310053, China

²ZJU-ENS Joint Laboratory of Medicinal Chemistry, College of Pharmaceutical Sciences, Zhejiang University, Hangzhou 310058, China

³Department of Medicinal Chemistry, College of Pharmaceutical Science, Zhejiang Chinese Medicinal University, Hangzhou 310053, China

*Corresponding author: Wenting Du, ddwttt@163.com

By inspiration of good Akt1 inhibitory and cytotoxic activity of our previously screened hits **1** and **2**, a series of novel benzopyrans **3a–c**, **4** and phenylpyrazoles **5a–c**, **6a–b**, and **7** were designed, synthesized, and biologically evaluated for their *in vitro* Akt1 inhibitory and cytotoxic activity. The results revealed that all of these compounds showed moderate-to-excellent anti-proliferative effects against the tested cancer cell lines (i.e. HL-60, OVCAR, PC-3, and HepG2). Among them, compounds **3a** and **3c** exhibited preferable Akt1 inhibitory activities (IC₅₀ of **3a** and **3c** are 6.18 and 5.28 μM , respectively), while compounds **4**, **5a–c**, **6a–b**, and **7** only showed weak Akt1 inhibitory activities. Consequently, we used molecular docking and dynamic simulation to propose a mode of binding between Akt1 and the **3c** compound.

Key words: Akt1, benzopyran, cytotoxic activities, molecular docking, phenylpyrazole

Received 12 July 2014, revised 13 October 2014 and accepted for publication 16 November 2014

Akt (also known as protein kinase B or PKB) acts as a central node in the PI3K/Akt/mTOR signaling pathway that plays an essential role in cellular survival, proliferation, growth, motility, and apoptosis (1). Akt can be classified into three subfamilies (Akt1, Akt2, and Akt3) that share a high degree of overall homology and similar downstream targets (2). Aberrant activation of Akt is associated with various malignancies such as breast, prostate, ovarian, and skin cancers (3,4); thus, Akt has been identified as a significant target for cancer treatment (5–7). Numerous

studies have demonstrated the importance of the Akt enzyme as a target in anticancer strategies—resulting in the identification of structurally diverse Akt inhibitors (e.g. HT-89). Many of these inhibitors are currently under clinical trial (e.g. perifosine, MK2206, triciribine, and GDC0068) (Figure 1) (8–14). Top-line results of phase I/II trials of MK2206 (15) and phase II trials of perifosine (16) indicate a bright future for the development of Akt inhibitors (17). However, there are still some issues needing to be addressed, such as drug resistance and toxicology. Consequently, the development of innovative Akt inhibitors with novel structures and mechanisms is very important. Previously, we combined a pharmacophore model with molecular docking in a virtual screening, resulting in identification of two benzopyrans **1** and **2** (Figure 2A) with favorable Akt1 inhibitory activities (IC₅₀ value of **1** and **2** are 5.4 and 3.9 μM , respectively) (18). It is noteworthy that these two compounds are multihydroxyl flavonoids, which are well-known natural products exhibiting extensively biological activities (including anticancer) and very low toxic properties (19,20). Thus, further optimization of this series of compounds as Akt inhibitors would lead to the discovery of multifunctional anticancer agents.

In this study, we aimed to enhance the Akt inhibitory activities of lead compounds **1** and **2** by performing structural optimizations. For clarity, the binding modes between Akt1 and compound **1** are presented in 2D structure (Figure 2B). Key interactions are described as follows: (i) catechol moiety of compound **1** forms two hydrogen bonds to the kinase hinge through residues Ala230 and Glu228, (ii) 5-hydroxyl group of chromanone ring hydrogen bonds with basic amino Lys179 of Akt1, and (iii) the prenyl moiety forms a hydrophobic interaction with residue Phe161. Thus, several clues for further structural optimization of these lead compounds are clearly given. Herein, we explored the effect of replacing the side chain (prenyl group) of compound **1** (morpholine **3a**, piperidine **3b**, benzylamine **3c**) extending the tolerance of side chain of compound **1**. Subsequently, we replaced the catechol moiety with a pyridyl ring (see compound **4**) based on the observed activity of compound **3c** and the reported potency of Akt inhibitors bearing a pyridine in the hinge region (21). Moreover, we extended the diversity of target compounds' skeleton by directly transferring flavones in the presence of hydrazine

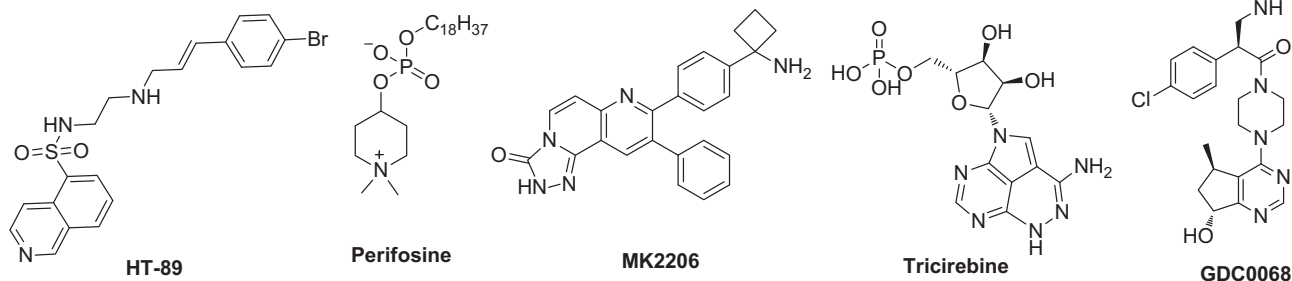


Figure 1: Structures of HT-89 and typical Akt inhibitors in clinical trials.

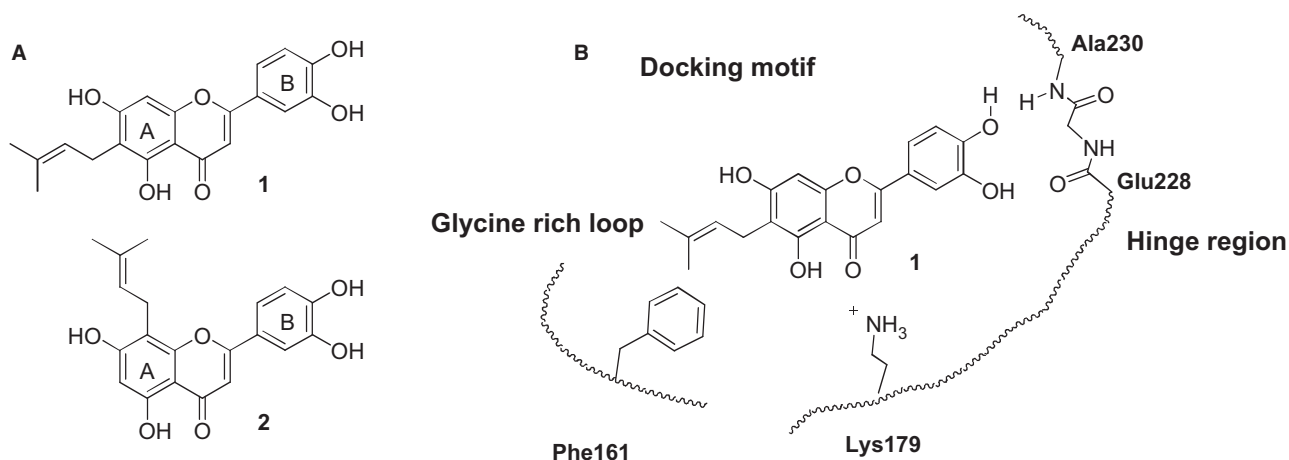


Figure 2: (A) Structure of screened hits **1** and **2** as Akt1 inhibitors in our previous study; (B) the interaction mode between compound **1** and Akt1 by proposed by docking study.

onto phenylpyrazole, another good mimic skeleton of flavonoid. Accordingly, compounds **3a-c**, **4**, **5a-c**, **6a-b**, and **7** (Figure 3) were synthesized and biologically evaluated for *in vitro* Akt1 inhibitory and cytotoxic activity against HL-60, OVCAR-8, PC-3, and HepG2 cell lines (22,23). Furthermore, the molecular docking and molecular dynamics/molecular mechanics (MD/MM) simulations were performed to investigate the proposed mode of interaction.

Experimental Section

Chemistry

¹H NMR spectra were recorded on a 500 MHz spectrometer (Brüker AM, Hangzhou, China), ¹³C NMR spectra were recorded on a 125 MHz spectrometer (Brüker AM) with TMS as the internal standard. The chemical shifts were expressed as δ values in parts in million (ppm) relative to tetramethylsilane (TMS). Melting points were obtained on a B-540 Büchi melting point apparatus and are uncorrected. Mass spectra were recorded on an Esquire-LC-00075 spectrometer. Reagents and solvents were purchased from commercial sources (Sigma-Aldrich, Alfa Aesar, TCI, Hangzhou, China and others).

General procedure of the synthesis of **3a-c**

To a solution of quercetin (0.2 mmol) in 2 mL isopropanol were added the corresponding amines (0.2 mmol) and paraformaldehyde (0.6 mmol), and the reaction mixture was heated to 60 °C for 5 h. After the reactants were consumed, EtOAc (30 mL) and 2N HCl aqueous solution (30 mL) was added to the mixture, then the pH of the aqueous phase was adjusted to seven by addition of 1N NaHCO₃ aqueous solution and extracted with EtOAc (3 × 15 mL). The combined organic layers were dried over Na₂SO₄, concentrated under vacuum, and purified by Buchi Sepacore preparative chromatography using RP-18 reverse-phase column to afford the title compounds.

2-(3,4-Dihydroxyphenyl)-3,5,7-trihydroxy-6-(morphinomethyl)-4H-chromen-4-one (**3a**)

Reagents: quercetin (60.4 mg, 0.2 mmol), morpholine (17.4 mg, 0.2 mmol), and paraformaldehyde (16.8 mg, 0.6 mmol). The product was obtained as a pale yellow solid (18%), m.p. >220 °C. ¹H NMR (DMSO-*d*₆) δ 12.53 (s, 1H), 7.72 (s, 1H), 7.60 (d, *J* = 8.5 Hz, 1H), 6.90 (d, *J* = 8.5 Hz, 1H), 6.22 (s, 1H), 3.82 (s, 2H), 3.59 (t, 4H),

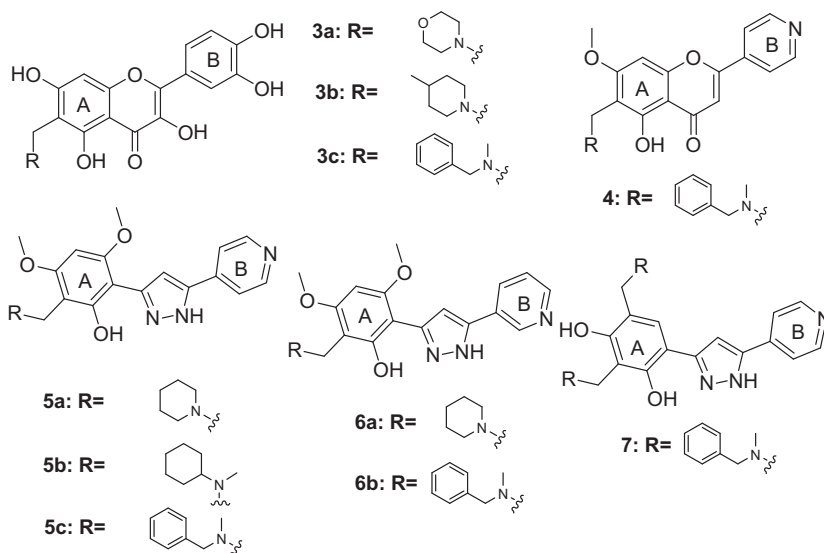


Figure 3: Structures of the newly designed benzopyrans and phenylpyrazoles as Akt inhibitors.

2.53 (t, 4H). ^{13}C NMR (100 MHz, DMSO) δ 175.97, 163.47, 159.54, 153.96, 147.69, 146.58, 145.09, 135.66, 122.21, 119.94, 115.61, 115.04, 102.87, 100.20, 97.93, 66.09, 52.72, 50.93. ESI-MS: m/z $[\text{M} - \text{H}]^-$ 400. HR-MS (ESI): Calcd. for $[\text{M} + \text{H}]^-$: 400.1032, found: 400.1028.

2-(3,4-Dihydroxyphenyl)-3,5,7-trihydroxy-6-((4-methylpiperidin-1-yl)methyl)-4H-chromen-4-one (3b)

Reagents: quercetin (60.4 mg, 0.2 mmol), 4-methylpiperidine (19.8 mg, 0.2 mmol), and paraformaldehyde (16.8 mg, 0.6 mmol). The product was obtained as a pale yellow solid (21%), m.p. >220 °C. ^1H NMR (DMSO- d_6) δ 7.68 (d, $J = 8.3$ Hz, 1H), 7.55 (dd, $J = 8.5, 2.1$ Hz, 1H), 6.90 (d, $J = 8.5$ Hz, 1H), 6.10 (s, 1H), 3.96 (s, 2H), 2.99 (d, $J = 11.5$ Hz, 2H), 2.29 (t, $J = 11.1$ Hz, 2H), 1.68 (d, $J = 12.0$ Hz, 2H), 1.53–1.35 (m, 1H), 1.16 (td, $J = 14.5, 3.1$ Hz, 2H), 0.91 (d, $J = 6.5$ Hz, 3H). ESI-MS: m/z $[\text{M} - \text{H}]^-$ 412. HR-MS(ESI): Calcd. for $[\text{M} + \text{H}]^-$: 412.1396, found: 412.1391.

6-((Benzyl(methyl)amino)methyl)-2-(3,4-dihydroxyphenyl)-3,5,7-trihydroxy-4H-chromen-4-one (3c)

Reagents: quercetin (60.4 mg, 0.2 mmol), *N*-methylbenzylamine (19.8 mg, 0.2 mmol), and paraformaldehyde (16.8 mg, 0.6 mmol). The product was obtained as a pale yellow solid (15%), m.p. >220 °C. ^1H NMR (MeOH- d_4) δ 7.74 (s, 1H), 7.58 (d, $J = 6.6$ Hz, 1H), 7.47–7.24 (m, 5H), 6.87 (d, $J = 10.3$ Hz, 1H), 6.12 (s, 1H), 4.16 (s, 1H), 3.88 (s, 2H), 2.41 (s, 2H). ESI-MS: m/z $[\text{M} - \text{H}]^-$ 434. HR-MS(ESI): Calcd. for $[\text{M} + \text{H}]^-$: 434.1240., found: 434.1245.

The general procedure for the synthesis of 12a-c

To a mixture of appropriate acetophenone **9** (10.2 mmol), isonicotinic acid or nicotinic acid (10.2 mmol) in pyridine (30 mL) was added POCl_3 (11.2 mmol) slowly at 0 °C. The reaction was stirred at room temperature for 16 h, then the reaction mixture was poured into water (100 mL), and the solid was separated by filtration and dried to give **10**. Subsequently, to a solution of the compound **10** in DMF was added potassium hydroxide (30.6 mmol) and the mixture stirred for 2 h, afterward, the reaction mixture was treated with ethyl acetate and water, and extracted by ethyl acetate (3×50 mL). The combined organic extraction was dried over Na_2SO_4 and concentrated to give crude residue **11**, which was further dissolved in acetic acid (10 mL) and conc. H_2SO_4 (1 mL). The reaction mixture was heated to 100 °C for 2 h, then diluted with water, neutralized with a saturated aqueous NaHCO_3 solution, extracted by ethyl acetate and finally purified by column chromatography on silica gel using petroleum ether-ethyl acetate as eluant to afford desired product.

5,7-Dimethoxy-2-(pyridin-4-yl)-4H-chromen-4-one (12a)

The product was obtained as a white solid (42%). ^1H NMR (CDCl_3) δ 8.79 (d, $J = 6.0$ Hz, 2H), 7.73 (d, $J = 6.0$ Hz, 2H), 6.78 (s, 1H), 6.59 (d, $J = 2.1$ Hz, 1H), 6.41 (d, $J = 2.1$ Hz, 1H), 3.97 (s, 3H), 3.93 (s, 3H). ESI-MS: m/z $[\text{M} + \text{H}]^+$ 284.

5,7-Dimethoxy-2-(pyridin-3-yl)-4H-chromen-4-one (12b)

The product was obtained as a white solid (58%). ^1H NMR (CDCl_3) δ 9.28 (d, $J = 1.0$ Hz, 1H), 8.75 (dd, $J = 4.8, 1.0$ Hz, 1H), 8.55–8.43 (m, 1H), 7.60 (dd, $J = 6.4, 3.8$ Hz,

1H), 6.70 (s, 1H), 6.54 (d, $J = 2.5$ Hz, 1H), 6.42 (d, $J = 2.5$ Hz, 1H), 4.02 (s, 3H), 3.95 (s, 3H). ESI-MS: m/z $[M + H]^+$ 284.

7-(Benzyloxy)-2-(pyridin-3-yl)-4H-chromen-4-one (12c)

The product was obtained as a white solid (61%). ^1H NMR (CDCl_3) δ 9.16 (brs, 1H), 8.77 (brs, 1H), 8.16 (dd, $J = 8.4$, 2.9 Hz, 2H), 7.42 (m, 6H), 7.10 (dd, $J = 8.8$, 2.3 Hz, 1H), 7.06 (d, $J = 2.2$ Hz, 1H), 6.79 (s, 1H), 5.21 (s, 2H). ESI-MS: m/z $[M + H]^+$ 330.

General procedure for the synthesis of 13a and 13b

To a solution of compound **12a** (1.0 mmol) in anhydrous CH_3CN (10 mL), anhydrous AlCl_3 (4.0 mmol) was added at room temperature, and then the mixture was refluxed overnight. The reaction mixture was poured into ice water, adjusted the pH ~ 6 using aqueous Na_2CO_3 , and then extracted with ethyl acetate (3×20 mL). The combined organic phases were washed with brine, dried over anhydrous Na_2SO_4 , concentrated and purified on silica gel to give desired product.

5-Hydroxy-7-methoxy-2-(pyridin-4-yl)-4H-chromen-4-one (13a)

The product was obtained as white solid (75%). ^1H NMR (500 MHz, CDCl_3) δ 12.50 (s, 1H), 8.83 (d, $J = 4.5$ Hz, 2H), 7.74 (d, $J = 4.5$ Hz, 2H), 6.77 (s, 1H), 6.53 (s, 1H), 3.90 (s, 3H). ESI-MS: m/z $[M + H]^+$ 270.

5-Hydroxy-7-methoxy-2-(pyridin-3-yl)-4H-chromen-4-one (13b)

The product was obtained as white solid (81%). ^1H NMR (500 MHz, CDCl_3) δ 12.44 (s, 1H), δ 9.23 (d, $J = 1.0$ Hz, 1H), 8.70 (dd, $J = 4.8$, 1.0 Hz, 1H), 8.52–8.40 (m, 1H), 7.62 (dd, $J = 6.5$, 4.0 Hz, 1H), 6.77 (s, 1H), 6.53 (s, 1H), 3.90 (s, 3H). ESI-MS: m/z $[M + H]^+$ 270.

Synthesis of 6-((benzyl(methyl)amino)methyl)-5-hydroxy-7-methoxy-2-(pyridin-4-yl)-4H-chromen-4-one 4

To a solution of **12a** (0.1 mmol) in 2 mL dioxane were added *N*-methylbenzylamine (0.1 mmol) and paraformaldehyde (0.3 mmol), and the mixture was stirred at 60 °C overnight. After cooling, water (5 mL) was added and extracted with ethyl ether (3×5 mL). The combined organic layers were dried over Na_2SO_4 and concentrated under vacuum. The residue was purified on silica gel to afford the title compound **4** as white solid (56%). ^1H NMR (500 MHz, CDCl_3) δ 8.82 (d, $J = 6.0$ Hz, 2H), 7.74 (d, $J = 6.1$ Hz, 2H), 7.43–7.15 (m, 5H), 6.78 (s, 1H), 6.52 (s, 1H), 3.90 (s, 3H), 3.64 (s, 2H), 2.26 (s, 2H). ^{13}C NMR

(101 MHz, DMSO) δ 182.05, 164.57, 160.59, 159.17, 156.71, 150.67, 139.32, 137.97, 128.60, 127.92, 126.68, 119.89, 109.28, 107.68, 104.95, 90.81, 61.41, 56.34, 47.43, 41.50. ESI-MS: m/z $[M + H]^-$ 403.

General procedure for the synthesis of 14a–14b

To a solution of compound **12** (2.0 mmol) in MeOH (10 mL), hydrazine hydrate (10.0 mmol) was added and the mixture was refluxed for 10 h. The reaction mixture was then poured into ice water and extracted with ethyl acetate (3×20 mL). The organic phase was washed with brine, dried over anhydrous Na_2SO_4 , and then concentrated in vacuum. The residue was purified by column chromatography on silica gel using petroleum ether-ethyl acetate as eluant to give desired product.

3,5-Dimethoxy-2-(5-(pyridin-4-yl)-1H-pyrazol-3-yl)phenol (14a)

Reagents: **12a** (566 mg, 2.0 mmol) and hydrazine hydrate (320 mg, 10.0 mmol). The product was obtained as white solid (76%). ^1H NMR (500 MHz, CDCl_3) δ 8.71 (d, $J = 6.0$ Hz, 2H), 7.58 (d, $J = 6.0$ Hz, 2H), 7.36 (s, 1H), 6.26 (d, $J = 2.3$ Hz, 1H), 6.16 (d, $J = 2.3$ Hz, 1H), 3.96 (s, 3H), 3.83 (s, 3H). ESI-MS: m/z $[M + H]^-$ 298.

3,5-Dimethoxy-2-(5-(pyridin-3-yl)-1H-pyrazol-3-yl)phenol (14b)

Reagents: **12b** (566 mg, 2.0 mmol) and hydrazine hydrate (320 mg, 10.0 mmol). The product was obtained as white solid (88%). ^1H NMR (500 MHz, $\text{MeOH-}d_4$) δ 8.99 (s, 1H), 8.50 (d, $J = 4.8$ Hz, 1H), 8.24 (d, $J = 8.0$ Hz, 1H), 7.52 (dd, $J = 7.8$, 4.9 Hz, 1H), 7.22 (s, 1H), 6.22 (d, $J = 2.3$ Hz, 1H), 6.20 (d, $J = 2.3$ Hz, 1H), 3.93 (s, 3H), 3.81 (s, 3H). ESI-MS: m/z $[M + H]^-$ 298.

Synthesis of 4-(5-(pyridin-4-yl)-1H-pyrazol-3-yl)benzene-1,3-diol 16

To a solution of **12c** (658 mg, 2.0 mmol) in MeOH (10 mL), hydrazine hydrate (320 mg, 10.0 mmol) was added and refluxed for 10 h. The reaction mixture was then poured into ice water and extracted with ethyl acetate (3×20 mL). The organic phase was washed with brine, dried over anhydrous Na_2SO_4 , and then concentrated in vacuum. The residue was purified by column chromatography on silica gel using petroleum ether-ethyl acetate as eluant to give solid. Then, a solution of the above solid and 5% Pd/C (30.0 mg) in EtOH was charged with hydrogen and refluxed overnight. The mixture was filtered and the filtrate was concentrated to give **16** without purification (48%, two steps). ^1H NMR (500 MHz, $\text{MeOH-}d_4$) δ 9.00 (brs, 1H), 8.48 (brs, 1H), 8.24 (brs, 1H), 7.52 (d, $J = 8.0$ Hz, 2H), 7.04 (s, 1H), 6.41 (d, $J = 8.0$ Hz, 2H). ESI-MS: m/z $[M + H]^-$ 254.

General procedure for the synthesis of compounds 5a–c, 6a, b, and 7

To a solution of **14** (or **16**) (0.1 mmol) in 2 mL dioxane were added corresponding amine (0.1 mmol) and paraformaldehyde (0.3 mmol), and the mixture was stirred at 60 °C overnight. After cooling to room temperature, the mixture was poured into water (5 mL) and extracted with ethyl acetate (3 × 5 mL). The combined organic layers were dried over anhydrous Na₂SO₄, concentrated and purified by column chromatography on silica gel using petroleum ether-ethyl acetate to afford the desired product.

3,5-Dimethoxy-2-(piperidin-1-ylmethyl)-6-(5-(pyridin-4-yl)-1H-pyrazol-3-yl) phenol (5a)

Reagent: **14a** (29.7 mg, 0.1 mmol), piperidine (8.5 mg, 0.1 mmol), paraformaldehyde (84 mg, 0.3 mmol). The product was obtained as white solid (55%), m.p. 178–180 °C. ¹H NMR (500 MHz, CDCl₃) δ 8.62 (d, *J* = 5.9 Hz, 2H), 7.80 (d, *J* = 6.1 Hz, 2H), 7.34 (s, 1H), 6.11 (s, 1H), 3.98 (s, 3H), 3.84 (s, 3H), 3.81 (s, 2H), 1.75–1.61 (m, 4H), 0.93–0.80 (m, 6H). ESI-MS: *m/z* [M + H]⁺ 395.

2-((Cyclohexyl(methyl)amino)methyl)-3,5-dimethoxy-6-(5-(pyridin-4-yl)-1H-pyrazol-3-yl) phenol (5b)

Reagent: **14b** (29.7 mg, 0.1 mmol), *N*-methylcyclohexylamine (11.3 mg, 0.1 mmol), paraformaldehyde (84 mg, 0.3 mmol). The product was obtained as white solid (52%), m.p. 165–166 °C. ¹H NMR (500 MHz, CDCl₃) δ 8.63 (d, *J* = 6.0 Hz, 2H), 7.81 (d, *J* = 4.8 Hz, 2H), 7.34 (s, 1H), 6.10 (s, 1H), 4.00 (s, 3H), 3.94 (s, 2H), 3.85 (s, 3H), 2.65–2.68 (m, 1H), 2.35 (s, 3H), 1.93–1.97 (m, 2H), 1.85–1.89 (m, 2H), 1.68–1.72 (m, 1H), 1.44–1.36 (m, 2H), 1.16–1.12 (m, 1H), 0.83–0.88 (m, 2H). ESI-MS: *m/z* [M + H]⁺ 423.

2-((Benzyl(methyl)amino)methyl)-3,5-dimethoxy-6-(5-(pyridin-4-yl)-1H-pyrazol-3-yl)phenol (5c)

Reagent: **14c** (29.7 mg, 0.1 mmol), *N*-methylbenzylamine (12.1 mg, 0.1 mmol), paraformaldehyde (84 mg, 0.3 mmol). The product was obtained as white solid (44%), m.p. 182–185 °C. ¹H NMR (500 MHz, CDCl₃) δ 8.63 (d, *J* = 5.6 Hz, 2H), 7.81 (d, *J* = 5.6 Hz, 2H), 7.39–7.29 (m, 5H), 7.26 (s, 1H), 6.14 (s, 1H), 3.99 (s, 3H), 3.89 (s, 2H), 3.86 (s, 3H), 2.28 (s, 3H). ESI-MS: *m/z* [M + H]⁺ 431.

3,5-Dimethoxy-2-(piperidin-1-ylmethyl)-6-(5-(pyridin-3-yl)-1H-pyrazol-3-yl) phenol (6a)

Reagent: **14b** (29.7 mg, 0.1 mmol), piperidine (8.5 mg, 0.1 mmol), paraformaldehyde (84 mg, 0.3 mmol). The product was obtained as white solid (59%), m.p. 183–185 °C. ¹H NMR (500 MHz, acetone-*d*₆) δ 9.11 (d,

J = 1.5 Hz, 1H), 8.49 (dd, *J* = 4.7, 1.6 Hz, 1H), 8.22 (dt, *J* = 7.9, 1.9 Hz, 1H), 7.39 (dd, *J* = 7.9, 4.8 Hz, 1H), 7.33 (s, 1H), 6.35 (s, 1H), 4.00 (s, 3H), 3.88 (s, 3H), 3.85 (s, 2H), 3.58 (s, 4H), 1.74–1.65 (m, 4H), 1.55 (s, 2H). ESI-MS: *m/z* [M + H]⁺ 395.

2-((Benzyl(methyl)amino)methyl)-3,5-dimethoxy-6-(5-(pyridin-3-yl)-1H-pyrazol-3-yl)phenol (6b)

Reagent: **14b** (29.7 mg, 0.1 mmol), *N*-methylbenzylamine (12.1 mg, 0.1 mmol), paraformaldehyde (84 mg, 0.3 mmol). The product was obtained as white solid (45%), m.p. 171–173 °C. ¹H NMR (500 MHz, acetone-*d*₆) δ 12.34 (brs, 1H), 9.09 (s, 1H), 8.48 (dd, *J* = 4.7, 1.5 Hz, 1H), 8.21 (dt, *J* = 7.9, 1.9 Hz, 1H), 7.44–7.36 (m, 5H), 7.35 (s, 1H), 7.32 (t, *J* = 7.0 Hz, 1H), 6.40 (s, 1H), 4.02 (s, 3H), 3.91 (s, 5H), 3.74 (s, 2H), 2.29 (s, 3H). ¹³C NMR (101 MHz, DMSO) δ 157.81, 157.68, 157.48, 157.41, 150.41, 150.02, 129.33, 128.47, 127.54, 119.40, 103.90, 99.18, 87.18, 60.00, 55.66, 55.60, 45.59. ESI-MS: *m/z* [M + H]⁺ 431.

2,4-bis((benzyl(methyl)amino)methyl)-6-(5-(pyridin-4-yl)-1H-pyrazol-3-yl) benzene-1,3-diol 7

Reagent: **16** (25.4 mg, 0.1 mmol), *N*-methylbenzylamine (24.2 mg, 0.2 mmol), paraformaldehyde (112 mg, 0.4 mmol). The product was obtained as a white solid (39%), m.p. 110–113 °C. ¹H NMR (500 MHz, CDCl₃) δ 8.66 (d, *J* = 5.8 Hz, 2H), 7.78 (d, *J* = 6.0 Hz, 1H), 7.46–7.30 (m, 11H), 6.87 (s, 1H), 4.00 (s, 2H), 3.79 (s, 4H), 3.64 (s, 2H), 2.35 (s, 3H), 2.27 (s, 3H). ESI-MS: *m/z* [M + H]⁺ 520.

Akt1 inhibitory activity assay

In vitro kinase assays were carried out using HTScan[®] PKB/Akt1 Kinase Assay kit (Cell Signaling Technology). Active recombinant Akt1 kinase (GST fusion protein, 4 ng) in 8 μL of 2.5× kinase buffer [62.5 mM Tris-HCl (pH 7.5), 25 mM MgCl₂, 12.5 mM β-glycerophosphate, 0.25 mM Na₃VO₄, 5 mM dithiothreitol (DTT)] was mixed with 2 μL of dimethyl sulfoxide (DMSO) vehicle or each of the compound (indicated concentrations), incubated at room temperature for 5 min, and 10 μL of ATP/substrate cocktail (20 mM ATP, 3 mM eNOS served as substrate) was added. After incubation at room temperature for 30 min, add 20 μL of 50 mM ethylenediaminetetraacetic acid (EDTA) (pH 8.0) and terminate the reaction. Then, PKB/Akt1 kinase activity was analyzed according to the manufacturer's instructions.

Cytotoxic activity assay

The cytotoxic activity of tested compounds in PC3, OV-CAR-8, HepG2, and HL-60 cells was measured using the MTT (3-(4,5-Dimethylthiazol-2-yl)-2,5-diphenyltetrazolium bromide, a tetrazole) assay (23). Cells were seeded in

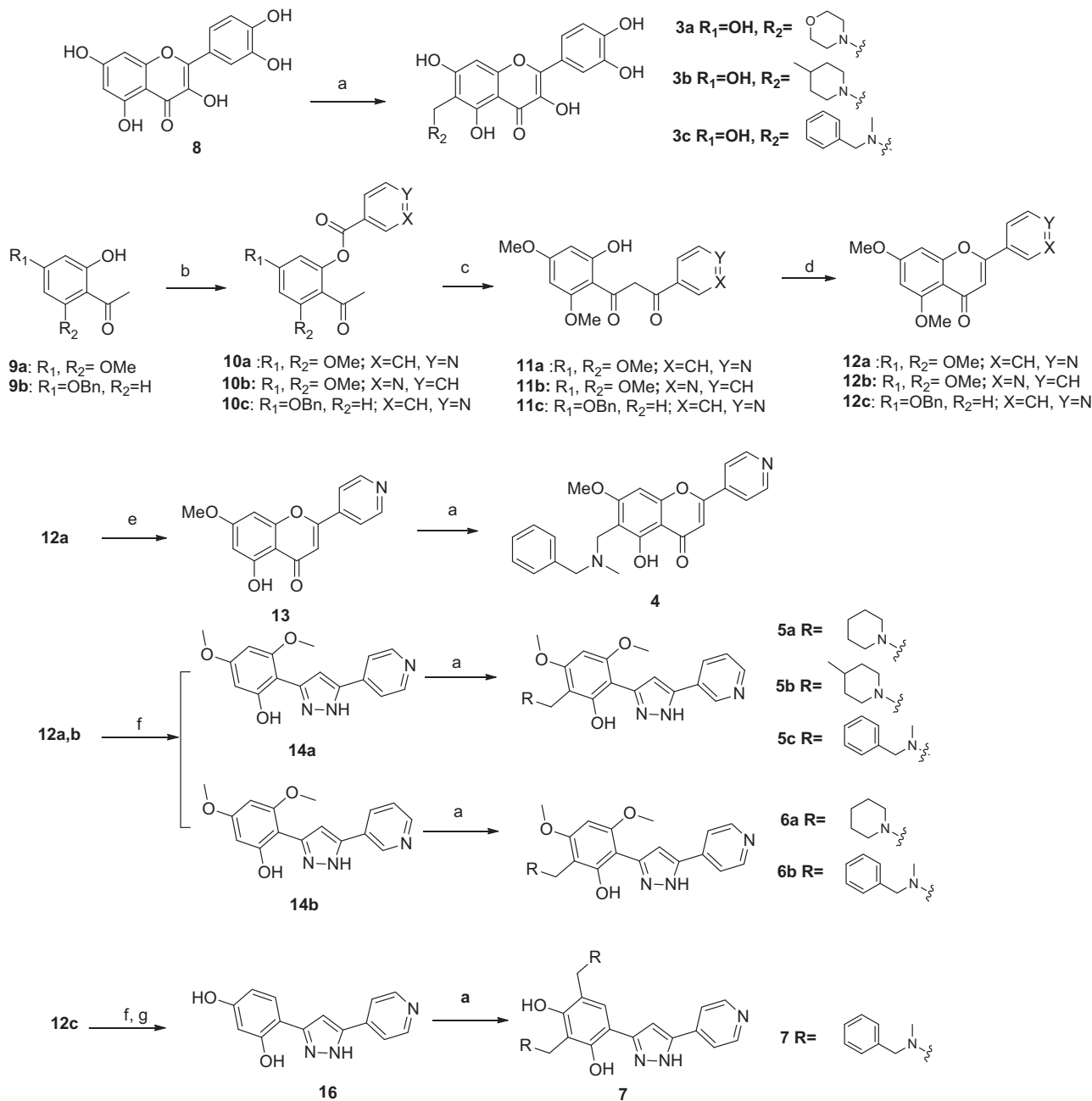
96-well microtiter plates (at a density of 4000 cells per well) for overnight attachment and exposed to each of the compound (1.0–100.0 μM) for 72 h. The MTT solution (5.0 mg/mL in RPMI 1640 medium; Sigma-Aldrich) was added (20.0 μL /well), and plates were incubated for a further 4 h at 37 °C. The purple formazan crystals were dissolved in 100.0 μL of DMSO. After 5 min, the plates were read on an automated microplate spectrophotometer (Bio-Tek Instruments, Winooski, VT, USA) at 570 nm. Assays were performed in triplicate on three independent

experiments. The concentration of drug inhibiting 50% of cells (IC_{50}) was calculated using the GraphPad prism software with microcomputers.

Computational Methods

Molecular docking with LigandFit

The X-ray crystal structure of Akt1 (PDB ID: 3OCB) was retrieved from the Protein Data Bank (PDB, <http://www.pdb.org>).



Scheme 1: The synthetic routes for compounds **3a–c**, **4**, **5a–c**, **6a–b**, and **7**. (a) paraformaldehyde, appropriate amine, isopropanol or dioxane. (b) nicotinic acid (or isonicotinic acid), pyridine, POCl_3 ; (c) KOH , DMF ; (d) HOAc , H_2SO_4 ; (e) AlCl_3 , CH_3CN ; (f) Hydrazine hydrate, EtOH ; (g) Pd/C , H_2 , EtOH .

pdb.org). The docking site of Akt1 was derived using the LigandFit site search utility in DISCOVERY STUDIO 2.5 software (Accelrys, Inc., San Diego, CA, USA). For the generation of different ligand conformations, we used variable numbers of Monte Carlo simulations. All the calculations during the docking step were performed under PLP Force Field formalism (24). A short rigid body minimization was then performed, and 50 poses for each ligand were saved. Scoring was performed with a set of scoring functions implemented in LigandFit module, including Dock_score (25), PLP1 (24), and PMF (26). The combination of consensus scoring method (27) and key interaction with the residues of Akt1 was applied to select the preferable output docking conformation.

Molecular dynamic and mechanical (MD/MM) simulation

With an aim to examine the reliability of the interaction mode between Akt1 and its inhibitor, the ligand-bound Akt1 complex proposed by LigandFit was further refined by MD/MM simulation: (i) An NVT ensemble molecular dynamic simulations with CHARMM force field were then performed at a constant temperature of 300 K with a time step of 1 fs for a total of 3 ns; (ii) then, the output conformation was initially run with CHARMM force field for 500 iterations of steepest descents, followed by a 500 iterations conjugate gradients optimization. The other parameters of MD/MM simulation were maintained at their Discovery studio default configuration.

Results and Discussion

Chemistry

The synthetic routes for compounds **3a–c**, **4**, **5a–c**, **6a–b**, and **7** are outlined in Scheme 1. According to the literature (28), the C-6 regioselective products **3a–c** can be obtained by a direct Mannich reaction on quercetin **8** in the presence of paraformaldehyde and corresponding amines (e.g. morpholine, 4-methylpiperidine, and *N*-methylbenzylamine) in

ethanol. In addition, esterification of hydroxyacetophenone **9** with carboxyl-pyridine (e.g. nicotinic acid and isonicotinic acid) yielded ester **10**. Diketone **11** was obtained by a Baker–Venkataraman rearrangement from **10**. Thereafter, efficient acid-promoted cyclization of **11** afforded flavone **12**. Also, demethylation of **12a** using aluminum chloride in anhydrous acetonitrile furnished **13**, and compounds **12a–b** were treated with hydrazine hydrate in ethanol to give phenylpyrazoles **14a–b**. Furthermore, compound **12c** was reacted with hydrazine hydrate and then debenzoylation using Pd/C/H₂ in ethanol to afford compound **16**. Finally, target compounds **4**, **5a–b**, **6a–b**, and **7** were obtained by a direct Mannich reaction on compounds **13**, **14a–b**, and **16** in the presence of paraformaldehyde and corresponding amines (e.g. *N*-methylbenzylamine, *N*-methylcyclohexylamine, piperidine) in dioxane.

Pharmacology

The target compounds **3a–c**, **4**, **5a–c**, **6a–b**, and **7** were tested for *in vitro* cytotoxic activity against four human cancer cell lines (i.e. HL60, OVCAR-8, PC-3, and HepG2). **H-89**, a well-known Akt inhibitor (29), was employed as a positive control. The results are summarized in Table 1. All of them exhibited moderate-to-potent cytotoxic activity. In the benzopyran class (**3a–c**), the effect of the side chain (Mannich base moieties) on the A-ring of benzopyran to the cytotoxic activity indicated that the *N*-methylbenzyl group (**3c**) was better than morpholine (**3a**) and piperidine (**3b**) in the matter of cytotoxic activity. As exemplified in compound **3c**, its IC₅₀ values against HL60, OVCAR-8, PC-3, and HepG2 cell lines were 7.56, 16.69, 15.45 and 7.2 μM, respectively. In the phenylpyrazole class, the effect of the side chain (Mannich base moieties) on A-ring of phenylpyrazole to the cytotoxic activity indicated that 4-methylpiperidine was preferable compared with the activity of compounds **5a–c**. In addition, the two Mannich base groups on A-ring of phenylpyrazole skeleton (i.e. compound **7**) attenuated the cytotoxic activity. The cytotoxic activity against solid tumor cells of compound **5b**, the most potent one, was observed to be significantly

Table 1: The cytotoxic activities of compounds **3a–c**, **4**, **5a–c**, **6a–b**, and **7** against HL-60, OVCAR-8, PC-3, and HepG2 cells

Compound	Cytotoxic activities (IC ₅₀ , μM)			
	HL-60	OVCAR-8	PC-3	HepG2
3a	16.65 ± 1.5	>50	42.74 ± 3.8	12.50 ± 0.9
3b	14.22 ± 1.1	>50	32.28 ± 2.2	18.57 ± 1.1
3c	7.56 ± 0.4	16.69 ± 2.0	15.45 ± 1.8	7.20 ± 0.5
4	13.32 ± 1.5	9.69 ± 0.9	30.13 ± 5.0	6.68 ± 0.4
5a	10.63 ± 1.2	13.94 ± 1.5	32.26 ± 4.1	22.18 ± 1.5
5b	4.75 ± 0.5	7.96 ± 0.8	4.98 ± 0.6	4.62 ± 0.5
5c	16.53 ± 1.4	9.73 ± 1.1	48.52 ± 10.5	20.47 ± 1.8
6a	11.64 ± 1.0	17.59 ± 1.9	>50	17.86 ± 1.5
6b	4.34 ± 0.3	10.76 ± 1.7	22.11 ± 2.5	10.26 ± 1.1
7	17.33 ± 1.2	38.00 ± 3.2	17.01 ± 1.2	>50
HT-89	11.45 ± 0.9	7.74 ± 0.5	9.49 ± 0.8	10.17 ± 0.6

Table 2: The Akt1 inhibitory activities of compounds **3a–c**, **4**, **5a–c**, **6a–b**, and **7**

Compound	IC ₅₀ (Inhibitory rate, %) ^a
3a	6.2 ± 0.4 μM
3b	(39%) ^a
3c	5.5 ± 0.5 μM
4	N. A. ^b
5a	(16%) ^a
5b	(19%) ^a
5c	(16%) ^a
6a	(23%) ^a
6b	(21%) ^a
7	(20%) ^a
H-89	1.7 ± 0.2 μM

^aThe Akt1 inhibitory rate was determined at a concentration of 10 μM.

^bN. A. means no activity.

Table 3: The docking results of compounds **3a–c**

Compound	Dock_score	-PLP1	-PMF
3a	94.17	99.86	88.51
3b	98.26	103.66	95.72
3c	104.31	108.64	73.68

improved when compared to lead compound **1** (IC₅₀ = 14.6, 23.8 for PC-3, OVCAR-8, respectively) in all cell lines except HL-60 cells (IC₅₀ = 4.98 and 7.96 for PC-3 and OVCAR-8, respectively).

The Akt1 inhibitory activity of screened hits was evaluated using HTScan[®] Akt1 Kinase Assay kit (Cell Signaling Technology, Beverly, MA, USA) with **H-89** as a positive

control. The results are presented in Table 2. Compounds **3a** and **3c** showed the best Akt1 inhibitory activities (IC₅₀ = 6.2 and 5.5 μM for **3a** and **3c**, respectively), which were comparable to our previously screened hits **1** and **2**; these results suggest that the introduction of more flexible substituents into A-ring of benzofuran was tolerated for Akt1 inhibitory activities. Besides, although compounds **4**, **5a–c**, **6a–b**, and **7** showed comparable cytotoxic activity with **3a–c**, the *in vitro* Akt1 inhibitory activities were weak (the inhibitory rate is between 15.9% and 23.1% at a concentration of 10 μM), indicating other possible targets contributing to their favorable cytotoxic activity. The study of phenylpyrazoles on their potential targets is ongoing.

Molecular docking and MD/MM simulation

With the aim to study the interaction mode between the active compounds **3a–c** and Akt1, all of them were docked into the active pocket of Akt1. The docking scores from various functions (Dock_score, PLP1 and PMF) are presented in Table 3. All of them showed good consensus results and good performance in various scoring functions. For example, the scores from Dock_scores, PLP1 and PMF for compound **3c** were 104.3, 108.6, and 73.7, respectively. Furthermore, the proposed complex of Akt1 and **3c** was then submitted for MD/MM simulation by DISCOVERY STUDIO 2.5 program, providing us with a stable compound **3c**-Akt1 complex. As shown in Figure 4A, compound **3c** was embraced in the Akt1 binding pocket. The polar and hydrophobic interaction between Akt1 and **3c** is presented in Figure 4B. The Glu228 and Ala230 residues of Akt1 in the hinge region made key hydrogen bond interactions with the catechol group of **3c**. An additional

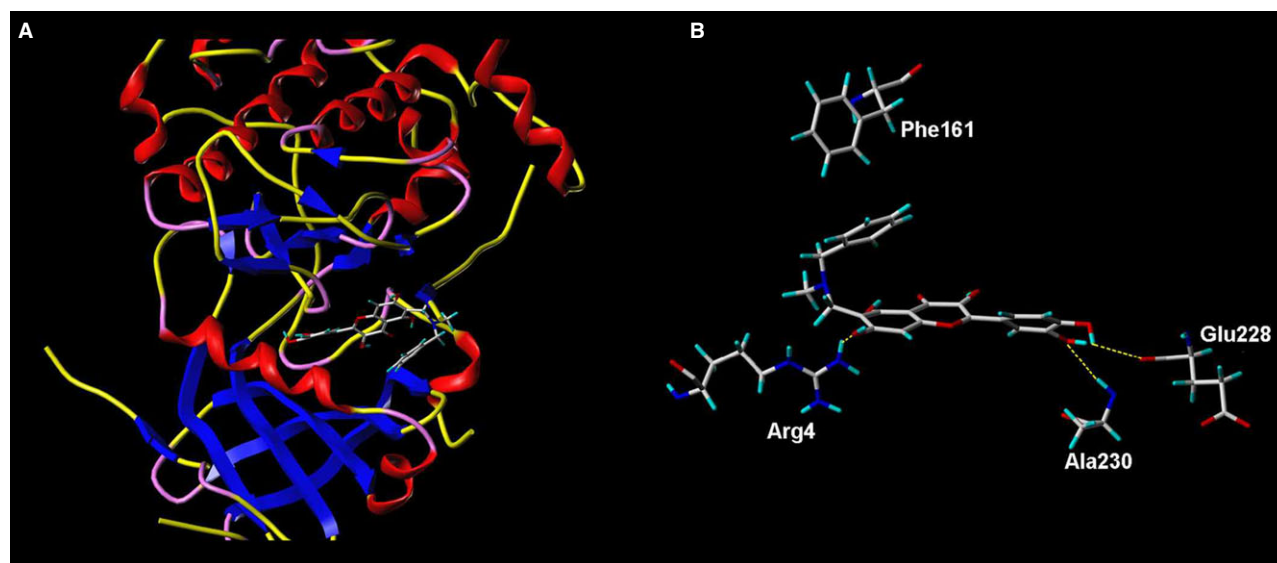


Figure 4: (A) Interaction mode of **3c** with Akt1: Compound **3c** was embraced in the Akt1 binding pocket; (B) compound **3c** is displayed in stick within the binding pocket of Akt1 in the detailed picture, and the hydrogen bond interactions between **3c** and Akt1 are highlighted using dash line.

hydrogen bond was observed between guanidine of Arg4 and 5-hydroxyl of **3c**. Besides, the benzyl moiety of **3c** packed into the glycine-rich pocket of Akt1, forming a π - π stacking interaction with Phe161 of Akt1.

Conclusion

In this study, a series of Mannich base of benzopyran and phenylpyrazole derivatives were designed, synthesized, and biologically evaluated for *in vitro* Akt1 inhibitory and cytotoxic activity. Most of them exhibited moderate-to-potent cytotoxic activity against four cancer cell lines. Moreover, three compounds **3a-c** showed promising Akt1 inhibitory activity that was comparable to that of lead compounds **1** and **2**. However, the Akt1 inhibitory activity of the other compounds was very weak. The negative relationship between cytotoxicity and Akt1 inhibitory activity strongly suggests that there are other mechanisms contributing to cancer cell apoptosis. In fact, determining the exact mechanism of action for these compounds is an ongoing project to give us a novel anchor point for further development of these series of compounds as anticancer agents. This is the first example, to the best of our knowledge, of extensive structural modification of flavonoids in the development of Akt1 inhibitors. Furthermore, the structural acquirement and the binding mode proposed in this study will be valuable for the future development of more potent flavonoids derivatives as Akt1 inhibitors.

Acknowledgments

The authors are grateful to the support provided by the National Natural Science Foundation of China (No. 81001359), The Education Department of Zhejiang Province, the general research project (No. Y201431886), and the Research Foundation of Zhejiang Medical College (No. 2011B01). We are also grateful to the support provided by Zhejiang Provincial Program for the Cultivation of High-level Innovative Health Talents (2014) and The 151 Talents Project in new century in Zhejiang Province (the third level, 2011).

Conflict of Interest

The authors confirm that this article content has no conflict of interests.

References

1. Cheng J.Q., Lindsley C.W., Cheng G.Z., Yang H., Nicosia S.V. (2005) The Akt/PKB pathway: molecular target for cancer drug discovery. *Oncogene*;24:7482–7492.
2. Masure S., Haefner B., Wesselink J.J., Hoefnagel E., Mortier E., Verhasselt P., Tuytelaars A., Gordon R., Richardson A. (1999) Molecular cloning, expression and characterization of the human serine/threonine kinase Akt-3. *Eur J Biochem*;265:353–360.
3. Staal S.P. (1987) Molecular cloning of the akt oncogene and its human homologues AKT1 and AKT2: amplification of AKT1 in a primary human gastric adenocarcinoma. *Proc Natl Acad Sci USA*;84:5034–5037.
4. Joseph R.T., Alfonso B. (2001) AKT plays a central role in tumorigenesis. *Proc Natl Acad Sci USA*;98:10983–10985.
5. Zinda M.J., Johnson M.A., Paul J.D., Horn C., Konicek B.W., Lu Z.H., Sandusky G., Thomas J.E., Neubauer B.L., Lai M.T., Graff J.R. (2001) AKT-1, -2, and -3 are expressed in both normal and tumor tissues of the lung, breast, prostate, and colon. *Clin Cancer Res*;7:2475–2479.
6. Sourbier C., Lindner V., Lang H., Agouni A., Schordan E., Danilin S., Rothhut S., Jacqmin D., Helwig J., Massfelder T. (2006) The phosphoinositide 3-kinase/Akt pathway: a new target in human renal cell carcinoma therapy. *Cancer Res*;66:5130–5142.
7. Tokunaga E., Kataoka A., Kimura Y., Oki E., Mashino K., Nishida K., Koga T., Morita M., Kakeji Y., Baba H., Ohno S., Maehar Y. (2006) The association between Akt activation and resistance to hormone therapy in metastatic breast cancer. *Eur J Cancer*;42:629–635.
8. Reuveni H., Livnah N., Geiger T., Klein S., Ohne O., Cohen I., Benhar M., Gellerman G., Levitzki A. (2002) Toward a PKB inhibitor: modification of a selective PKA inhibitor by rational design. *Biochemistry*;41:10304–10314.
9. Lindsley C.W., Barnett S.F., Yaroschak M., Bilodeau M.T., Layton M.E. (2007) Recent progress in the development of ATP-competitive and allosteric Akt kinase inhibitors. *Curr Top Med Chem*;7:1349–1363.
10. Barnett S., Bilodeau M., Lindsley C.W. (2005) The Akt/PKB family of protein kinases: a review of small molecule inhibitors and progress towards target validation. *Curr Top Med Chem*;5:109–125.
11. Kondapaka S.B., Singh S.S., Dasmahapatra G.P., Sausville E.A., Roy K.K. (2003) Perifosine, a novel alkylphospholipid, inhibits protein kinase B activation. *Mol Cancer Ther*;2:1093–1103.
12. Hirai H., Sootome H., Nakatsuru Y., Miyama K., Taguchi S., Tsujioka K., Ueno Y., Hatch H., Majumder P.K., Pan B.S., Kotani H. (2010) MK-2206, an allosteric Akt inhibitor, enhances antitumor efficacy by standard chemotherapeutic agents or molecular targeted drugs *in vitro* and *in vivo*. *Mol Cancer Ther*;9:1956–1967.
13. Gloesenkamp C.R., Nitzsche B., Ocker M., Di Fazio P., Quint K., Hoffmann B., Scherubl H., Hopfner M. (2012) AKT inhibition by triciribine alone or as combination therapy for growth control of gastroenteropancreatic neuroendocrine tumors. *Int J Oncol*;40:876–888.
14. Blake J.F., Xu R., Bencsik J.R., Xiao D., Kallan N.C., Schlachter S., Mitchell I.S. *et al.* (2012) Discovery and preclinical pharmacology of a selective ATP-competitive Akt inhibitor (GDC-0068) for the treatment of human tumors. *J Med Chem*;55:8110–8127.

15. Yap T.A., Yan L., Patnaik A., Fearen I., Olmos D., Papadopoulos K., Baird R.D. *et al.* (2011) First-in-man clinical trial of the oral pan-AKT inhibitor MK-2206 in patients with advanced solid tumors. *J Clin Oncol*;29:4688–4695.
16. Cho D.C., Hutson T.E., Samlowski W., Sportelli P., Somer B., Richards P., Sosman J.A., Puzanov I., Michaelson M.D., Flaherty K.T., Figlin R.A., Vogelzang N.J. (2012) Two phase 2 trials of the novel Akt inhibitor perifosine in patients with advanced renal cell carcinoma after progression on vascular endothelial growth factor-targeted therapy. *Cancer*;118:6055–6062.
17. Holmes D. (2011) PI3K pathway inhibitors approach junction. *Nat Rev Drug Discov*;10:563–564.
18. Dong X., Zhou X., Jing H., Chen J., Liu T., Yang B., He Q., Hu Y. (2011) Pharmacophore identification, virtual screening and biological evaluation of prenylated flavonoids derivatives as PKB/Akt1 inhibitors. *Eur J Med Chem*;46:5949–5958.
19. Veitch N.C., Grayer R.J. (2008) Flavonoids and their glycosides, including anthocyanins. *Nat Prod Rep*;25:555–611.
20. Boudet A.M. (2007) Evolution and current status of research in phenolic compounds. *Phytochemistry*;68:2722–2735.
21. Li Q., Woods K.W., Thomas S., Zhu G., Packard G., Fisher J., Li T. *et al.* (2006) Synthesis and structure-activity relationship of 3',4'-bispyridinylethylenes: discovery of a potent 3-isoquinolinylopyridine inhibitor of protein kinase B (PKB/Akt) for the treatment of cancer. *Bioorg Med Chem Lett*;16:2000–2007.
22. Heerding D.A., Rhodes N., Leber J.D., Clark T.J., Keenan R.M., Lafrance L.V., Li M. *et al.* (2008) Identification of 4-(2-(4-amino-1,2,5-oxadiazol-3-yl)-1-ethyl-7-{{(3S)-3-piperidinylmethyl} oxy}-1H-imidazo[4,5-c]pyridin-4-yl)-2-methyl-3-butyn-2-ol (GSK690693), a novel inhibitor of AKT kinase. *J Med Chem*;51:5663–5679.
23. Dumble M., Crouthamel M.C., Zhang S.Y., Schaber M., Levy D., Robell K., Liu Q., Figueroa D.J., Minthorn E.A., Seefeld M.A., Rouse M.B., Rabindran S.K., Heerding D.A., Kumar R. (2014) Discovery of novel AKT inhibitors with enhanced anti-tumor effects in combination with the MEK inhibitor. *PLoS ONE*;9: e100880.
24. Gehlhaar D.K., Verkhivker G.M., Rejto P.A., Sherman C.J., Fogel D.B., Fogel L.J., Freer S.T. (1995) Molecular recognition of the inhibitor AG-1343 by HIV-1 protease: conformationally flexible docking by evolutionary programming. *Chem Biol*;2:317–324.
25. Venkatachalam C.M., Jiang X., Oldfield T., Waldman M. (2003) LigandFit: a novel method for the shape-directed rapid docking of ligands to protein active sites. *J Mol Graph Model*;21:289–307.
26. Muegge I., Martin Y.C. (1999) A general and fast scoring function for protein-ligand interactions: a simplified potential approach. *J Med Chem*;42:791–804.
27. Montes M., Miteva M.A., Villoutreix B.O. (2007) Structure-based virtual ligand screening with LigandFit: pose prediction and enrichment of compound collections. *Proteins*;68:712–725.
28. Chen L., Hu T.S., Zhu J., Wu H., Yao Z.J. (2006) Application of a regioselective mannich reaction on naringenin and its use in fluorescent labeling. *Synlett*;8: 1225–1229.
29. Kumar C.C., Madison V. (2005) AKT crystal structure and AKT-specific inhibitors. *Oncogene*;24:7493–7501.